

# **POLAROGRAPHIC OXYGEN SENSORS, THE OXYGRAPH, AND HIGH-RESOLUTION RESPIROMETRY TO ASSESS MITOCHONDRIAL FUNCTION**

ERICH GNAIGER

*Department of General and Transplant Surgery, D.Swarovski Research Laboratory, Medical University of Innsbruck, Innsbruck, Austria; Oroboros Instruments, Innsbruck, Austria*

- 1. Introduction**
- 2. Polarographic oxygen sensor and traditional oxygraphy**
- 3. High-resolution respirometry: the Oxygraph-2k**
  - 3.1. Calibration of polarographic oxygen sensors and oxygen concentration in respiration media at air saturation**
  - 3.2. From oxygraph slopes to respiratory flux corrected for background effects**
- 4. Phosphorylation control protocol with intact cells**
  - 4.1. Titration steps of the PC protocol**
  - 4.2. Experimental example for the PC protocol**
  - 4.3. Flux control ratios from the PC protocol**
- 5. Intact cells, permeabilized cells and tissue, or isolated mitochondria**
  - 5.1. Intact cells**
  - 5.2. Permeabilized cells and tissue**
  - 5.3. Isolated mitochondria**
- 6. Titration protocols in permeabilized cells, permeabilized tissue preparations, and isolated mitochondria**
- 7. Multisensor applications**

## 1. INTRODUCTION

Recent developments in high-resolution respirometry, combining advanced instrumentation with multiple substrate-uncoupler-inhibitor titration protocols, provide standardized and routine analyses of metabolic flux through various mitochondrial pathways. This technology allows assessments of membrane integrity (coupling of oxidative phosphorylation; cytochrome *c* release), of respiratory inhibition resulting from effects on the phosphorylation or on the electron transport systems, as well as activities of dehydrogenases, and metabolite transport across the inner mitochondrial membrane. These assessments are done via selective permeabilization of the cell membrane while leaving the mitochondrial membranes intact, or isolation of mitochondria, and can reveal acute drug effects on mitochondria. The use of intact cells limits the application of substrates, inhibitors and uncouplers to those that are permeable through the plasma membrane. On the other hand, use of intact cells offers the advantage of studying the control of oxidative phosphorylation under more physiological conditions and evaluating drug effects on mitochondrial function that might be mediated through complex cellular signaling pathways. Most applications of high-resolution respirometry use the measurement of oxygen in a closed system, which allows continuous monitoring of respiration in response to titrated compounds.

In this chapter, the new methodological standards set by high-resolution respirometry are discussed and compared with traditional polarographic methods. Also covered is potential multiplexing respirometry with sensors for simultaneous measurement of pH (proton flux, related to  $H^+/O$  ratios in isolated mitochondria, or acid production by glycolysis in intact cells), mitochondrial membrane potential (via cationic phenylphosphonium probes), nitric oxide (inhibition of respiratory complexes), and cytochrome spectra (redox state). Incorporating an electronically controlled titration-injection micropump provides the benefits of an open system, such as measurements at steady state and feedback control of experimental variables, while retaining the advantages of a closed system. The interested reader is encouraged to consult [www.orooboros.at](http://www.orooboros.at), where details of most of the protocols and assays described here are provided.

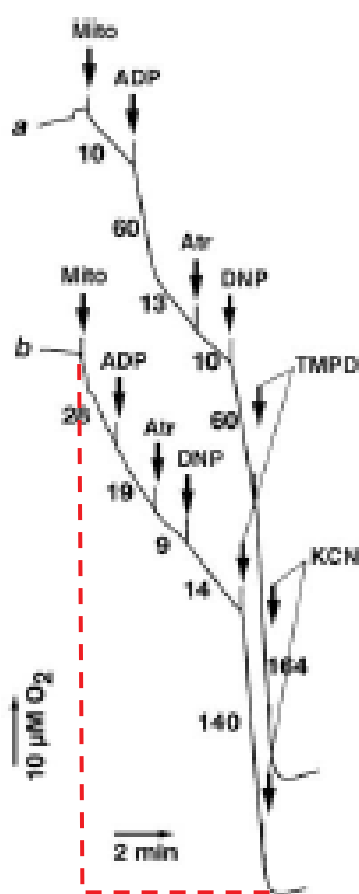
Mitochondrial dysfunction is implicated in a wide range of pathologies, including drug-induced organ toxicity and other adverse events. This sets new demands on standardization and routine screens for diagnosis of mitochondrial dysfunction, since limitations of traditional methods have frequently discouraged routine evaluation of mitochondrial liabilities within the drug development process [1] or in the clinical laboratory in general [2]. Defects in oxidative phosphorylation are generally studied by the measurement of mitochondrial oxygen consumption, where use of the polarographic oxygen sensor [3] has long replaced the classical manometric (Warburg) apparatus. High-resolution respirometry is, however, a comparatively recent development [4,5], which now provides a widely applicable tool for routine and specific analyses of mitochondrial function/dysfunction where (1) reliability and quality control are important (clinical studies, drug toxicity), (2) the amount of biological material is limited (cultured cells, tissue biopsies), (3) pathological effects result in reduced respiration, and (4) effects need to be tested at physiological, low intracellular oxygen levels [4-9].

Appart from the oxygraphic assay of cytochrome *c* oxidase activity [7] and activity measurements of other oxygen-consuming enzymes [10], diagnostic substrate-uncoupler-inhibitor titration protocols in mitochondrial respiratory studies [11-13] yield information on the capacities of metabolic pathways rather than individual enzymes, and thus provide insight into pathological effects on integrated mitochondrial function. It is well established that various defects in oxidative phosphorylation (*OXPHOS*) can be identified by the measurement of oxygen consumption (respirometric *OXPHOS* analysis) in fresh sample preparations that are not detected via more focused enzymatic analysis, via measurement of mitochondrial

membrane potential, or via electron microscopic analyses of mitochondrial structure [11]. This is not surprising, since respirometric *OXPHOS* analysis provides a screening approach that integrates structural and biochemical injuries of mitochondria that reflect not only derangement of membrane structure, but also defects of enzyme systems in membrane transport, dehydrogenases, electron transport, and coupled ADP phosphorylation. Although some drugs inhibit specific mitochondrial enzymes directly and hence yield mitochondrial cytopathies comparable to specific genetic defects [11,14], many drug-induced mitochondrial toxicities result from multiple impairments that may be more comparable to the complex pathological patterns observed in degenerative diseases [15], ageing [16,17], oxidative stress [18,19], ischemia-reperfusion injury [13] and apoptosis [20]. Small changes in cellular respiration, minor alterations in respiratory flux control ratios, and subtle differences in effects of drugs on respiration, particularly when the response is immediate, may indicate significant mitochondrial defects that reflect injuries of mitochondrial proteins or membranes. On longer time scales, such perturbations may reflect defects of mtDNA or alterations in mitochondrial and/or other cellular signaling cascades.

Assessment of *OXPHOS* in living and permeabilized cells, small amounts of tissue from transgenic animal models, human needle biopsies, and small numbers of isolated mitochondria requires high-resolution respirometry for accurate results. For example, high-resolution respirometry can be performed with less than 1 mg of fresh muscle tissue, fewer than 500,000 cells, or less than 0.05 mg of mitochondrial protein, which is 10-fold less than is required using conventional oxygraphic instruments.

## 2. POLAROGRAPHIC OXYGEN SENSOR AND TRADITIONAL OXYGRAPHY



The principle of respirometry in a closed chamber is based on monitoring oxygen concentration, which declines as the biological sample consumes oxygen. Plotting oxygen concentration over time (Figure 1) yields the oxygraph slope, which is in large measure related to oxygen consumption by the sample but is also confounded by undesired artifacts. The latter include instrumental background and are typically minimized by the instrumental hardware and/or corrected for by software according to standards established more than 10 years ago [4,5].

The oxygen concentration is measured by a Clark electrode (named after its inventor Leland Clark, a professor of chemistry at Antioch College), which contains a gold or platinum cathode and a Ag/AgCl anode separated

**Figure 1** Traces of oxygen concentration over time with traditional oxygraphy in an experiment with mitochondria isolated from mouse liver at 22 °C: curve a, freshly prepared; curve b, trehalose frozen. Addition of mitochondria, Mito (protein concentration 1 mg/mL); ADP, Atr (atractyloside), DNP, TMPD and KCN indicate various additions (arrows). Numbers indicate the negative slope [ $\mu\text{M}/\text{min}$ ]. (From Yamaguchi et al. [22], with permission from Macmillan. Copyright © 2007).

by concentrated KCl aqueous solution. Voltage is applied (~0.6 to 0.8 V) and these two half-cells are separated from the solution being monitored by a O<sub>2</sub>-permeant membrane, often Teflon, that excludes ions and other potential reductants. Dissolved O<sub>2</sub> diffuses from the solution through the membrane and is reduced to water by electrons at the cathode, yielding a hydroxide. The anode reaction is oxidation of Ag precipitating at the Ag/AgCl anode, providing a current that is proportional to O<sub>2</sub> partial pressure,  $p_{O_2}$ , in the experimental solution. These sensors are typically calibrated using air-saturated media, and dithionite for zero  $p_{O_2}$ . To convert  $p_{O_2}$  to oxygen concentration, the oxygen solubility of the medium must be known, which is a function of temperature and salt concentration. Although the physical configuration varies between various instruments, all require some means of regulating and maintaining constant temperature [3].

Traces of oxygen concentration as a function of time [21-24] (Figure 1) yield information that can be optimized when time derivatives and corrections for side effects are included, although respiratory flux techniques improve resolution substantially (Figure 2). Issues typical of traditional polarographic assessments can be discerned in most such traces and are described, along with their solutions, below.

1. *Signal stability.* Before addition of mitochondria into the chamber, instability of the oxygen signal indicates the possible magnitude of variation (Figure 1; trace *a*), which may be due to an initial equilibration process or to irregular sensor behavior. This would then exert a stronger influence on the initial portions of the experiment, and less so on later sections, when the system becomes progressively stable.

2. *Oxygen consumption of the sensor.* The contribution of oxygen-dependent oxygen consumption of the polarographic oxygen sensor is not quantified or may be within the limits of sensor instability. However, this signal is typically small compared to respiration and can be determined empirically.

3. *Linearity of the slope.* Within each metabolic state, linearity of the slope of oxygen over time is assumed (e.g., before addition of ADP in Figure 1; trace *b*), whereas observation of the time course of changes in respiration (resulting in nonlinear slopes) reveals important details of mitochondrial function (continuous loss of respiratory capacity in trace *b*, Figure 1).

4. *Time resolution.* Time-dependent responses to addition of substrates or drugs cannot be resolved in the time frame of experiments with high mitochondrial concentrations, due to rapid oxygen depletion of the medium.

5. *Limited time for titrations.* Oxygen concentrations drops by about 100  $\mu$ M or about 40 % air saturation within about 6 minutes after addition of mitochondria at high concentration (Figure 1), leaving little or no scope for experimental controls, such as stepwise titration of dinitrophenol (DNP) to evaluate the optimum uncoupler concentration at which flux is maximum (Figure 2; optimum uncoupler concentration may be different in mitochondria incubated with various drugs or after pretreatment of mitochondria).

6. *Oxygen back-diffusion.* After KCN titration, oxygen concentration increases steeply, due to back-diffusion of oxygen into the chamber at about 60 % air saturation. In the absence of autoxidation of *N,N,N',N'*-tetramethyl-*p*-phenylenediamine dihydrochloritde (TMPD) and ascorbate, back-diffusion would be even higher, indicating that this is a significant source of error for measuring respiration (e.g., after inhibition by atractyloside), even at relatively high oxygen levels and at high protein concentrations of mitochondria in the chamber (1 mg/mL).

7. *Chemical oxygen consumption.* Ascorbate and TMPD in mitochondrial respiration media show a high reactivity with oxygen due to autoxidation, which varies as a function of oxygen concentration. Correction of respiration for autoxidation is required to evaluate cytochrome c oxidase (CcOX) activity [7,25].

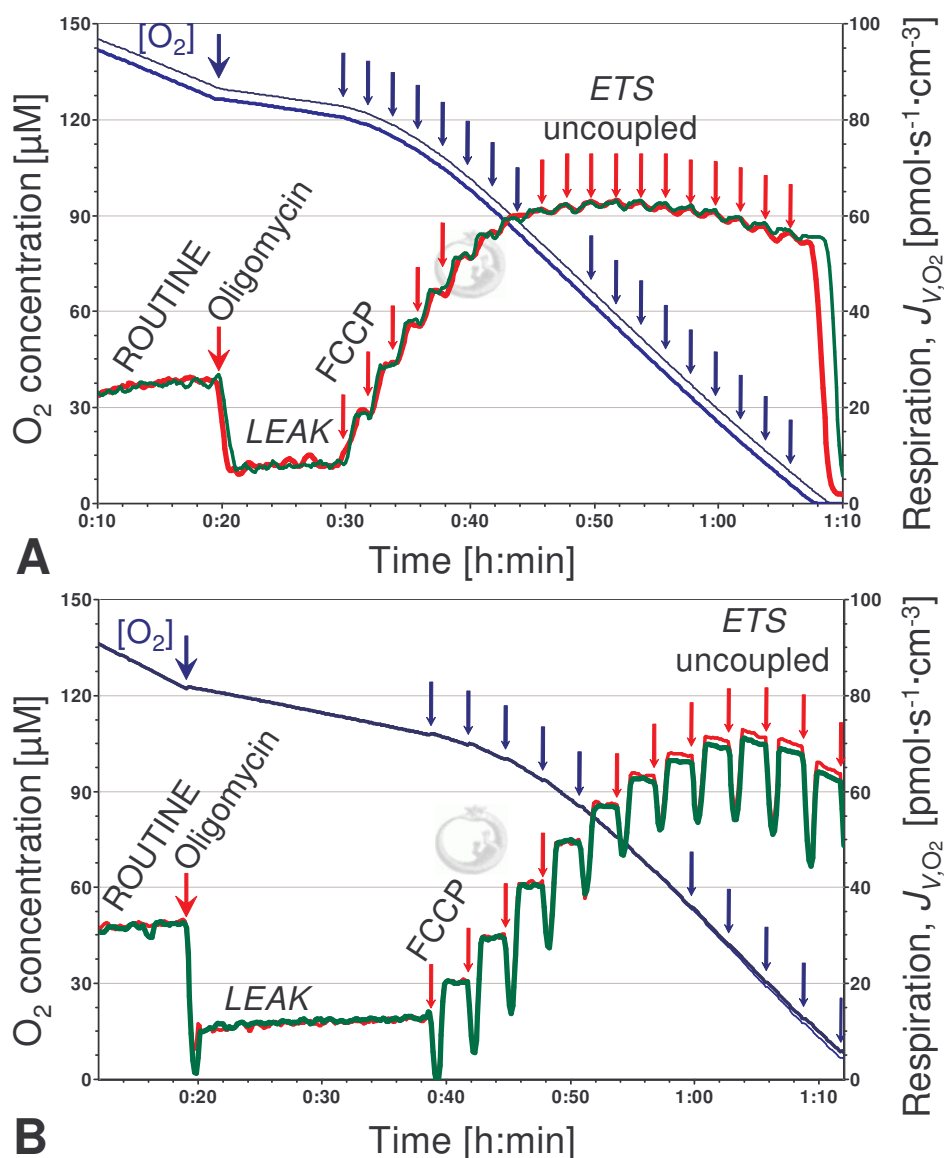


**Figure 2** High-resolution respirometry and phosphorylation control titration in intact cells. Superimposed plots of oxygen concentration  $[O_2]$  and respiration, calculated as the negative time derivative of oxygen concentration. Simultaneous replicate measurements in the left and right chamber ( $2\text{ cm}^3$ ) of the OROBOROS Oxygraph-2k are shown in each graph. Parental hematopoietic 32D cells were used at  $1.1 \cdot 10^6$  to  $1.5 \cdot 10^6$  cells/ $\text{cm}^3$ , suspended in culture medium RPMI at  $37^\circ\text{C}$  (ROUTINE respiration, *R*). Oligomycin ( $2\ \mu\text{g}\cdot\text{ml}^{-1}$ ; resting or LEAK state, *L*) is titrated manually ( $1\ \mu\text{l}$ ). After inhibition of ATP synthase, nonphosphorylating flux declines to a new steady state, although LEAK respiration tends to increase gradually with time. Uncoupler (FCCP) was titrated automatically with the TIP-2k, in steps of  $0.1$  ( $1.0$ )  $\mu\text{l}$ , adding  $10$  ( $1.0$ ) mM FCCP, corresponding to an increase in the final concentration of  $0.5\ \mu\text{M}$  FCCP in the Oxygraph-2k chamber. Downwards deflections of apparent flux are caused by the high oxygen concentration in ethanol and are stronger as the titrated volume is increased. The titration is fast ( $20$  and  $30\ \mu\text{l}/\text{s}$ ), at intervals of  $120$  ( $180$ ) s. Maximum uncoupled flux (capacity of the electron transport system, ETS; state *E*) was reached at  $5.5$  and  $4.5\ \mu\text{M}$  FCCP, and maximum sample dilution was  $<1\ \%$  when respiration was inhibited by higher FCCP concentrations. O2k experiments 2005-04-09 EF-03 (A) and 2005-09-14 EF-01 (B), carried out by participants of Oxygraph-2k courses.

Attempts to solve these problems by producing microchambers were largely counterproductive: Although the higher sample concentration in a smaller volume yields a higher volume-specific respiration, thus addressing problem 1 and 7 by increasing the ratio of mitochondrial respiration to signal drift and chemical autoxidation rate, the side effect (problem 2) of sensor consumption per volume increases as much as mitochondrial respiration per volume. Reduced sensor consumption can be achieved by application of microsensors, the stability of which declines with the reduction of cathode area [3]. Limitations 3 to 5 become more severe as sample concentration increases. Problem 6 relative to respiratory activity increases in microchambers due to the unfavourable surface-to-volume ratio. Since applications of microchambers [26-29] are restricted and problematic, or difficult to apply [30], a paradigm shift to a large chamber volume (2 cm<sup>3</sup>) was involved in the development of high-resolution respirometry for routine application with small amounts of sample, taking care to eliminate artifacts.

### 3. HIGH-RESOLUTION RESPIROMETRY: THE OXYGRAPH-2k

Several features distinguish high-resolution respirometry from traditional oxygraphs [5], combined in the new Oxygraph-2k (O2k, OROBOROS INSTRUMENTS, Innsbruck, Austria; Figure 3). The specifications are unique: the limit of detection of respiratory flux is 1 pmol·s<sup>-1</sup>·cm<sup>-3</sup> (0.001 μM·s<sup>-1</sup>) and the limit of detection of oxygen concentration extends to 0.005 μM O<sub>2</sub>. For the non-specialist, the O2k provides robustness and reliability of instrumental performance. With small amounts of sample and correspondingly low respiratory flux per volume, the oxygen capacity of the system is exhausted slowly, allowing sufficient time to evaluate the stability of respiratory activity in each metabolic state and to permit complex titration regimes in intact cells (Figure 2) or in permeabilized cells and tissues [13,16-20]. To increase throughput in research with cell cultures and in the pharmacological arena, user-friendly features make it possible to apply several instruments in parallel, each O2k with two independent chambers (Figure 3).

The chambers, sensors and electronics are shielded by a copper block and stainless steel housing (Figure 3). High long-term signal stability and low noise of the oxygen signal are a basis for online calculation of oxygen flux taken as the negative time derivative of oxygen concentration with high time resolution (Figure 2). Angular insertion of the oxygen sensor into the cylindrical chamber places the membrane-covered cathode of the polarographic oxygen sensor into an optimum position for stirring (Figure 3, inset). All materials in contact with the respiration medium are diffusion tight, with the glass chamber and PVDF or titanium stoppers (vs. Perspex), Viton O-rings, and magnetic stirring bars coated by PVDF or PEEK (vs. Teflon). In particular, Teflon, which has an oxygen solubility >10-fold that of aqueous media, is not feasible for high-resolution assays, due to long delays of oxygen back-diffusion from the Teflon material when oxygen declines in the closed chamber. Fully integrated instrumental control includes electronic Peltier temperature regulation (2 to 45 °C, stability at ±0.001 °C), stirrer control, and the automatic titration-injection micropump TIP-2k (not shown). Standardized calibration procedures of the oxygen signal, response time of the sensor, and instrumental or chemical background effects provide an experimental basis for high accuracy [5].

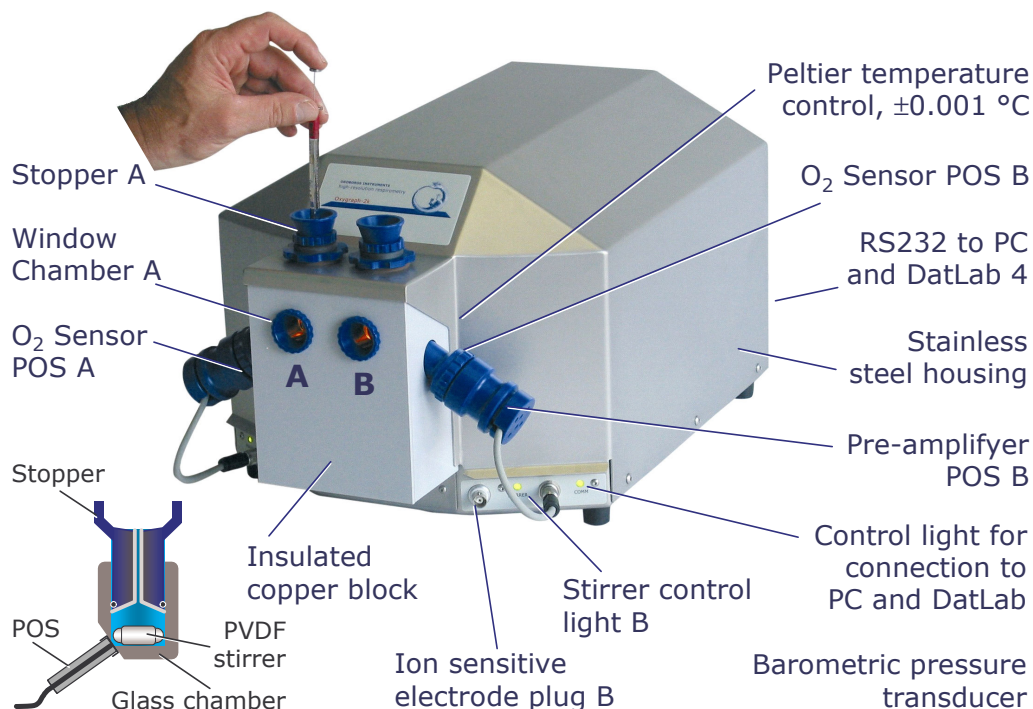


**Figure 3** Oxygraph-2k for high-resolution respirometry. Two identical and independent 2-ml glass chambers (A and B) are housed in an insulated copper block which is maintained at constant temperature by electronic Peltier temperature regulation. Oxygen concentration is recorded continuously by polarographic oxygen sensors (POS) in each chamber, which is sealed by a stopper containing a capillary for extrusion of gas bubbles and insertion of a needle for titrations. Additional holes through the stopper (PVDF) are made for insertion of various electrodes, the signals of which are simultaneously recorded by the DatLab software. The PVDF (or PEEK) stirrers are powered by electrically pulsed magnets inserted in the copper block. Data are processed online to calculate oxygen consumption of intact cells, permeabilized tissues, or isolated mitochondria (Copyright ©2005-2008 by OROBOROS INSTRUMENTS. Reproduced with permission; [www.orooboros.at](http://www.orooboros.at).)

### 3.1. Calibration of Polarographic Oxygen Sensors and Oxygen Concentration in Respiration Media at Air Saturation

The polarographic oxygen sensors (OROBOPoS) are stable for several months without exchange of membrane or electrolyte (Figure 4). This long-term stability of the polarographic oxygen sensors ensures that the O2k is ready to use. The amperometric measurement of oxygen by Clark-type polarographic oxygen sensors yields a current that is converted to a voltage and is strongly influenced by temperature [3]. Nevertheless, in the range from zero oxygen to pure oxygen at about 1 mM dissolved O<sub>2</sub>, modern polarographic instruments are superior to other technologies, such as optical sensors. This imposes high demands on the electronics; the digital resolution is 2 nM, yielding a 500,000-fold dynamic range. Air calibration is conveniently performed in an experimental medium at experimental temperature in the O2k chamber, providing a small gas phase of air and observing stabilization of the sensor signal as equilibration is reached between gas and the well-stirred aqueous phase ( $R_1$ ; Figure 5B). Oxygen calibration is fully supported by the software (DatLab, OROBOROS INSTRUMENTS, Innsbruck, Austria) and combines the following information:

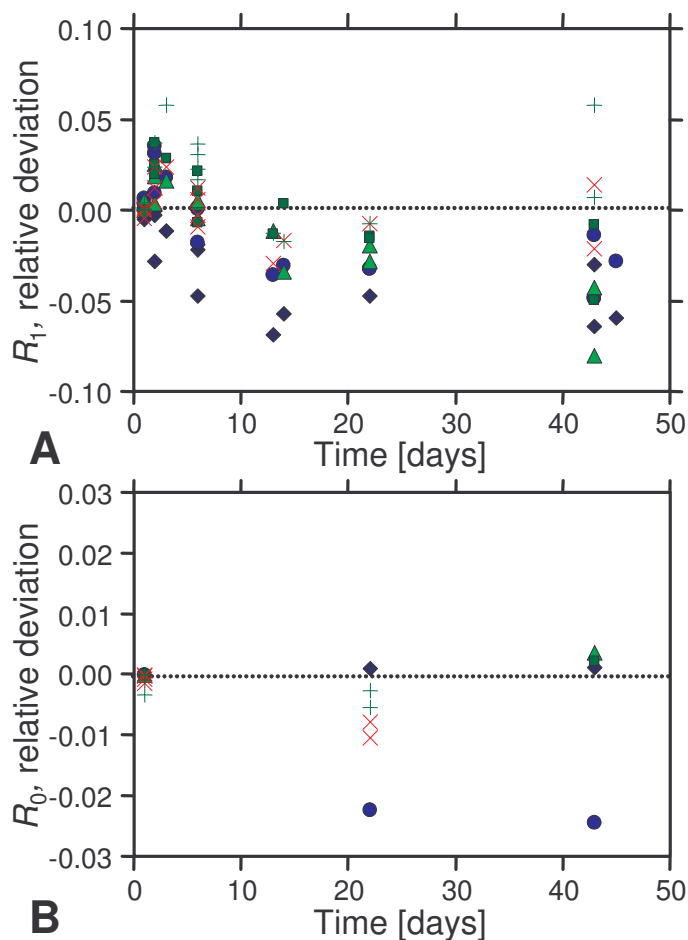


**Figure 4** Stability of the signals of six polarographic oxygen sensors, OROBoPOS, measured in separate chambers at air calibration,  $R_1$ , and zero calibration,  $R_0$ , over a period of >1 month at constant temperature (25 °C) but in different aqueous media, at stirrer speeds of 750 rpm or 300 rpm and with different stirrers (PEEK, PVDF, and small Viton-covered Teflon stirrer bars). Between experiments (isolated mitochondria and cell homogenates with typical substrate+uncoupler +inhibitor titrations), membranes were never exchanged and the sensors were left mounted to the O2k-chambers, which were filled with 70 % ethanol. Under such variable experimental conditions, daily air calibration improves the accuracy (A), whereas zero calibrations are not required at a regular basis for routine experiments (B). A: Relative deviation of  $R_1$  at time  $t$ , relative to day 1, is  $R_1(t)/R_1(1)-1$ . B: Relative deviation of  $R_0$  is  $R_0(t)/R_1(t)-R_0(1)/R_1(1)$ .  $R_0(1)/R_1(1)$  ranged from 0.02 to 0.14.

1. The raw signal,  $R_1$ , obtained at air saturation of the medium.
2. The experimental temperature,  $T$  [°C], measured in the thermoregulated copper block encasing the glass chambers.
3. The barometric pressure,  $p_b$  [kPa], measured by an electronic pressure transducer.
4. The oxygen partial pressure,  $p_{O_2}$  [kPa] in air saturated with water vapour, as a function of barometric pressure and temperature and the oxygen solubility,  $S_{O_2}$  [ $\mu\text{M}\cdot\text{kPa}^{-1}$ ] in pure water as a function of temperature, as calculated by the software [3].

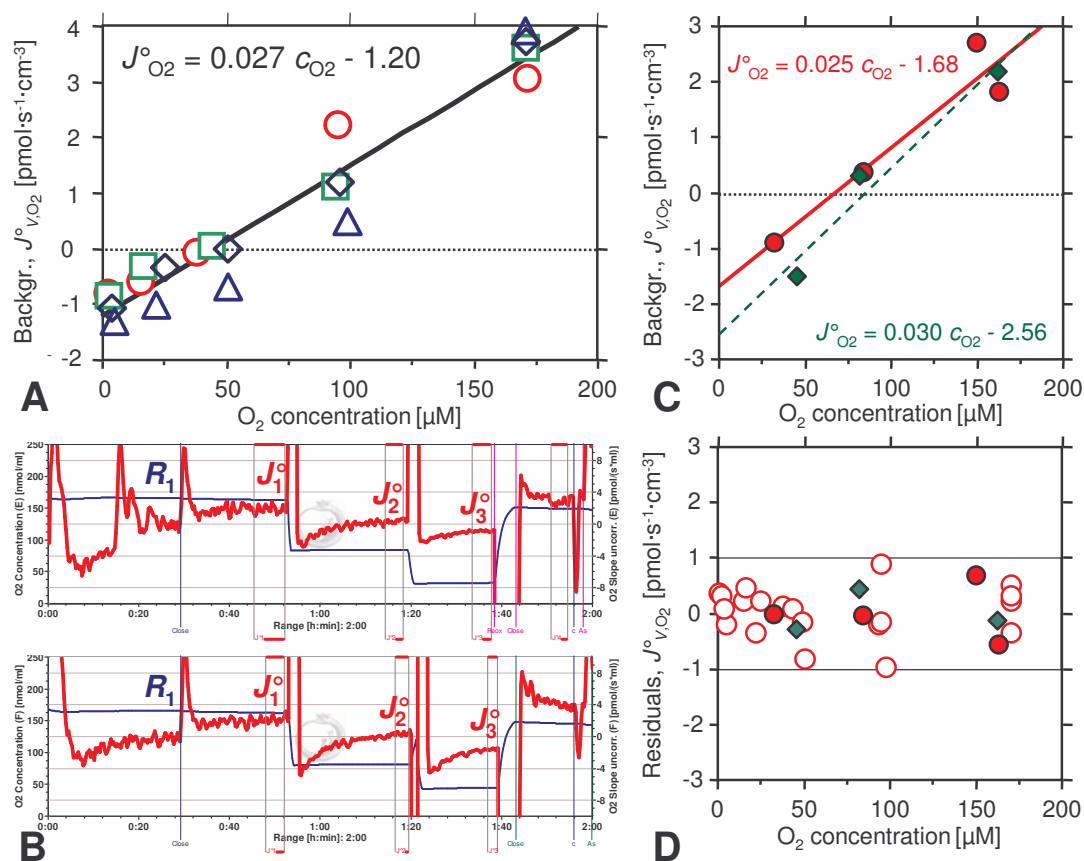


**Figure 5** Instrumental background oxygen flux measured in culture medium without cells at 37 °C in the Oxygraph-2k with a 2-cm<sup>3</sup> chamber volume. (A) Background test in four chambers under routine laboratory conditions (compare [12]). The regression line is calculated for all data points in the different chambers. (B) Background test performed by students during an O2k course. (C) Plot of instrumental background flux as a linear function of oxygen concentration, from traces shown in (B). (D) Deviation from the linear background regression [residuals from (A) and (C)], indicating the limit of detection of biological respiration at  $\pm 1$  pmol·s<sup>-1</sup>·cm<sup>-3</sup>, when the linear parameters are applied for automatic online correction of respiration.

5. The oxygen solubility factor of the incubation medium,  $F_M$ , which expresses the effect of the salt concentration on oxygen solubility relative to pure water, which must be known for accurate calibration. In mitochondrial respiration medium MiR05 (OROBOROS INSTRUMENTS; [31]),  $F_M$  is 0.92 determined at 30 and 37 °C [32], and  $F_M$  is 0.89 in serum at 37 °C [33]; we use the same factor for culture media such as RPMI, endothelial growth medium or Dulbecco's modified Eagle's medium. Air calibrations are best performed daily before starting an experiment.

6. The most convenient second calibration point,  $R_0$ , chosen at zero oxygen concentration. Occasional checks over a period of months are sufficient (Figure 4B), except in studies of oxygen kinetics, when short-term zero drift must be accounted for by internal zero calibration, for resolution in the nM oxygen range [4,5]. Zero oxygen is obtained when oxygen is depleted by mitochondrial respiration (Figure 2A) or when dithionite, Na<sub>2</sub>S<sub>2</sub>O<sub>4</sub>, is added for a fast zero calibration.

At standard barometric pressure (100 kPa), the oxygen concentration at air saturation is 207.3  $\mu$ M at 37 °C (19.6 kPa partial oxygen pressure). In MiR05 and serum, the

corresponding saturation concentrations are only 191 and 184  $\mu\text{M}$ . In bioenergetics, mitochondrial respiration may be given in the units  $\text{natom O}\cdot\text{s}^{-1}\cdot\text{cm}^{-3}$  and the dioxygen concentrations have to be multiplied by 2 to obtain  $\mu\text{M O}$  instead of  $\mu\text{M O}_2$ . Errors of 15 %, due to inaccurate oxygen solubility values, appear in the literature.

### 3.2. From Oxygraph Slopes to Respiratory Flux Corrected for Background Effects

Some sources of error in respiratory measurements with an oxygraph are due to the oxygen sensor. Linear sensor drift by 10 % per day, at 190  $\mu\text{M}$  at air saturation (37 °C), would amount to a slope of  $0.22 \text{ pmol}\cdot\text{s}^{-1}\cdot\text{cm}^{-3}$  ( $0.013 \mu\text{M}\cdot\text{min}^{-1}$ ). The long-term stability of the OROBoPOS (Figure 4A), presents no limitation for accuracy of the measurement of the flux. Thermal fluctuations at a temperature dependence of the signal of the POS of 3 % per °C [3] present a considerable problem: With thermal oscillations amounting to changes of 0.01 °C per minute, flux would fluctuate at  $\pm 1 \text{ pmol s}^{-1}\cdot\text{cm}^{-3}$  as a function of temperature. Improved temperature stability is therefore required for high-resolution respirometry (Figure 3) and for continuous display of smooth traces of respiratory flux (Figure 2). Since the signal of the polarographic oxygen sensor is sensitive to stirring of the aqueous medium, any irregular movements of the stirrer cause noise proportional to oxygen concentration. At low oxygen concentration, therefore, smaller absolute deviations are observed of oxygen concentration per unit of time, and the plot of oxygen flux becomes smoother (Figure 5B).

The lower oxygen consumption of microsensors is related to the low stirring sensitivity, but the generally lower signal-to-noise ratio renders oxygen microsensors not suitable for high-resolution respirometry. In addition to the function of the oxygen sensor, the properties of the oxygraph chamber influence the respirometric results. Standardized protocols for chamber calibration (instrumental background test) constitute an essential component of high-resolution respirometry, as they reduce instrumental artifacts. Consideration of oxygen back-diffusion is of major importance compared to correction for the oxygen consumption of the sensor [4,5,17].

The key study paving the way to measuring oxidative phosphorylation in isolated mitochondria [34] used a vibrating platinum microelectrode in a  $1 \text{ cm}^3$  cuvette that was not sealed against the air, with oxygen back-diffusion amounting to  $100\cdot 10^3 \text{ pmol}\cdot\text{s}^{-1}\cdot\text{cm}^{-3}$  after depletion of half of the oxygen dissolved at air saturation. The principle of a closed chamber could be applied when using high mitochondrial concentrations that lead to oxygen depletion within 120 to 200 s, corresponding to respiratory fluxes of  $800\cdot 10^3$  to  $2,000\cdot 10^3 \text{ pmol}\cdot\text{s}^{-1}\cdot\text{cm}^{-3}$  (20,000- to 50,000-fold above the average fluxes in Figure 2). If no correction for back-diffusion is applied, respiratory fluxes would include systematic errors of 5 to 12 % at 50 % air saturation under these conditions. Rates of back-diffusion in closed chambers are ideally zero, but this is difficult to achieve in practice. Back-diffusion at zero oxygen concentration in the  $2 \text{ cm}^3$  chamber is  $2 \pm 1 \text{ pmol}\cdot\text{s}^{-1}\cdot\text{cm}^{-3}$  with high-resolution respirometry [5], or  $4 \text{ pmol}\cdot\text{s}^{-1}$  into the chamber (Figure 5). This specification can be compared with few determinations of oxygen back-diffusion ranging from 10 to  $25 \text{ pmol}\cdot\text{s}^{-1}$  when extrapolated to zero oxygen concentration, in oxygraphs with volumes in the range of 1 to  $8 \text{ cm}^3$ , specifically designed for accurate measurements of P/O ratios or for studies at low oxygen levels [35-38]. With a progressive decline of oxygen concentration in the chamber, diffusion gradients increase and uncorrected back-diffusion of oxygen into the medium distorts the results.

In high-resolution respirometry, oxygen flux is background-corrected online as a continuous function of oxygen concentration [4,5]. Instrumental background is determined as a function of experimental oxygen concentration (Figure 5), and numerically calculated slopes are corrected on the fly for instrumental background by DatLab (Figure 2). A typical instrumental background experiment is shown in Figure 5B, starting with the standard protocol for air calibration of the oxygen sensor in experimental medium. Subsequent to

testing for O<sub>2</sub> sensor performance, the instrumental background test yields a calibration of the O<sub>2</sub>k chamber performance. When closing the chamber after equilibration at air saturation, oxygen diffusion into or out of the chamber is zero, and the oxygen consumption by the polarographic oxygen sensor can be measured (Figure 5B; first mark:  $J^{\circ}1$ ;  $3 \text{ pmol}\cdot\text{s}^{-1}\cdot\text{cm}^{-3}$ , owing to electrochemical oxygen reduction at the cathode). Oxygen consumption by the polarographic oxygen sensor increases linearly with oxygen pressure, whereas back-diffusion is maximum at zero oxygen and after rapid aerobic-anoxic transitions (Figure 5B). For reducing oxygen concentration rapidly, the stopper is lifted into a reproducible stopper position defined by a spacer, to obtain a gas phase above the stirred medium. After injecting a small volume of argon or nitrogen into this gas phase, the oxygen concentration in the medium drops quickly, and the stoppers are pushed gently into the chamber to extrude the entire gas phase. Flux stabilizes after an undershoot (Figure 5B), and the second mark,  $J^{\circ}2$ , is set on the section of stable flux. This is continued at one or two more reduced oxygen levels (Figure 5B; third mark:  $J^{\circ}3$ ). In this instrumental background test, oxygen back-diffusion is evaluated by following an overall time course of oxygen depletion (Figure 5B) which matches the time course of the decline of oxygen concentration in the actual experiment (Figure 2).

Plotting background oxygen flux as a function of oxygen concentration yields a fairly linear relation with intercept  $a^{\circ}$  and slope  $b^{\circ}$  (in Figure 5A,  $-1.2 \text{ pmol}\cdot\text{s}^{-1}\cdot\text{cm}^{-3}$  and  $0.027$ , respectively) [39]. These values are used (1) to confirm proper function of the respirometer (results are close to the default values of  $-2$  and  $0.025$ ), (2) to monitor the instrumental characteristics over time ( $a^{\circ}$  may become more negative suddenly or gradually over weeks of experiments, indicating an increasing leak, due possibly to a defective O-ring on the stopper that must be replaced), and (3) for online instrumental background correction of flux during respirometric experiments in the corresponding O<sub>2</sub>k chambers. Background-corrected oxygen consumption,  $J_{V,O_2}$  [ $\text{pmol}\cdot\text{s}^{-1}\cdot\text{cm}^{-3}$ ] is calculated as,

$$J_{V,O_2} = -1000\cdot dc_{O_2}/dt - (a^{\circ} + b^{\circ}\cdot c_{O_2}) \quad (1)$$

where  $c_{O_2}$  [ $\mu\text{M}$  or  $\text{nmol}\cdot\text{cm}^{-3}$ ] is oxygen concentration measured at time  $t$  [Equation (1)],  $dc_{O_2}/dt$  is the time derivative of oxygen concentration, and the expression in parentheses is the background oxygen flux.

Using high-resolution respirometry, experimental respiratory fluxes in resting states are typically about  $10 \text{ pmol}\cdot\text{s}^{-1}\cdot\text{cm}^{-3}$  (Figure 2), and corresponding background corrections amount to 20 % under these conditions (Figure 6). By comparison with traditional Clark sensor technology, atractyloside inhibited respiration is  $9 \mu\text{M}\cdot\text{min}^{-1}$  in Figure 1 ( $150 \text{ pmol}\cdot\text{s}^{-1}\cdot\text{cm}^{-3}$ ). Traditional oxygraphs using chambers or stoppers made of Perspex, Teflon stirrers, or sealings that are not diffusion-tight therefore require >10 times higher amounts of cells or mitochondria, and the problem of oxygen diffusion is further aggravated when the chamber volume is reduced. Due to the low residual oxygen consumption after inhibition by rotenone+antimycin A, the relative effect of instrumental background correction is large and highly oxygen dependent (Figure 6).

In polarographic determination of cytochrome *c* oxidase activity, ascorbate, TMPD and cytochrome *c* are used as substrates. Chemical autoxidation of these substrates is a function of substrate concentration and is strongly oxygen dependent. Chemical background oxygen flux is a linear function of oxygen concentration above 40-50  $\mu\text{M}$ , and corrections in the form of equation (1) can be applied online. The linear parameters  $a'$  and  $b'$  (chemical background, after correction for instrumental background) are characteristic for the chemical process in the particular medium. The mean  $\pm$ SD from six Oxygraph-2k chambers with MiR05 (three instruments operated in parallel by participants of an O<sub>2</sub>k teaching course) were:  $a' = 10.7\pm 1.4$  and  $b' = 0.24\pm 0.07$  [12].

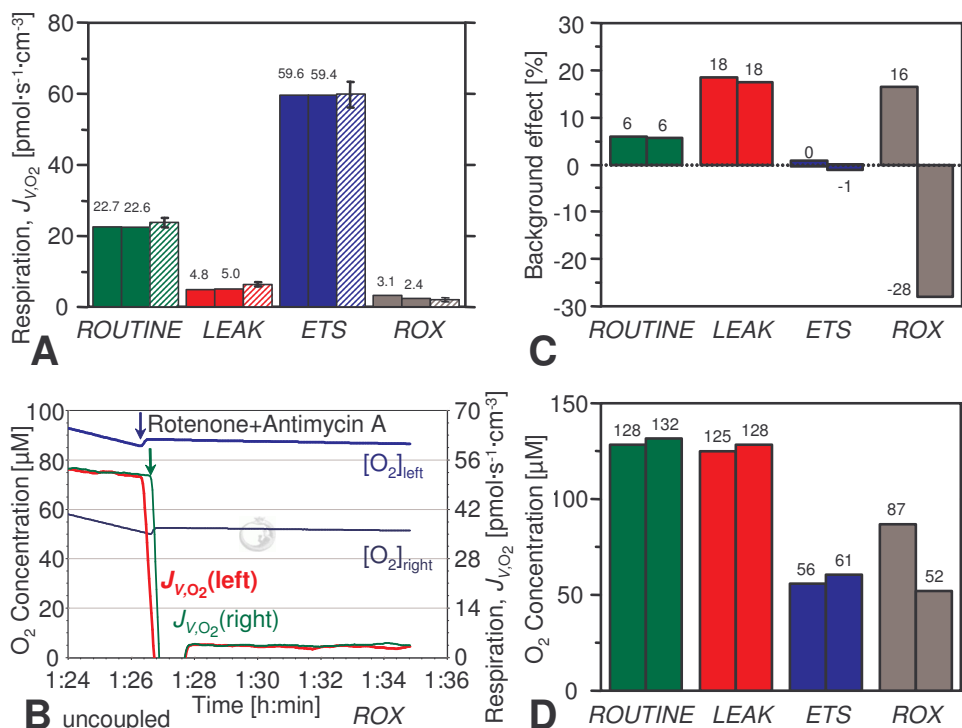


**Figure 6** Analysis of phosphorylation control by high-resolution respirometry. (A) Bar graph obtained online from marked sections of the experiment (solid bars with values, from the two chambers in Figure 2A), and means  $\pm$ SD (hatched bars) from six parallel runs. Respiration of intact cells in state *R* (ROUTINE), *L* (LEAK; oligomycin-inhibited) and *E* (ETS; uncoupled, at optimum FCCP concentration for maximum flux). In the inhibited state (rotenone+antimycin A), residual oxygen consumption, ROX, is in large part due to cellular, nonmitochondrial oxygen consumption. *R*, *L* and *E* are corrected for ROX. (B) Measurement of ROX (continuation of experiments of Figure 2A) after reoxygenation of the medium to different levels in the two chambers ( $[O_2]_{\text{left}}$  and  $[O_2]_{\text{right}}$ ). Flux was independent of oxygen concentration and declined progressively with time due to high, inhibitory FCCP concentrations, and was inhibited to a constant level after addition of rotenone+antimycin A. All results on respiration are corrected for instrumental background. C: Relative effect of instrumental background on respiratory flux (solid bars in A), as a function of average oxygen concentration measured during the respective time intervals (D).

#### 4. PHOSPHORYLATION CONTROL PROTOCOL WITH INTACT CELLS

A simple phosphorylation control protocol (PC-protocol) is described and interpreted for evaluation of the physiological respiratory control state of the intact cells, the mitochondrial coupling state, uncoupled respiratory capacity, and rotenone+antimycin A-sensitive respiration. Respiratory control states are induced in intact cells by application of specific membrane-permeable inhibitors and uncouplers (Figure 2). The initial incubation state is cellular ROUTINE respiration,  $C_R$ , reflecting physiological respiratory control. Cells may be suspended in a culture medium supporting ROUTINE respiration and growth by exogenous substrates ( $C_{GR}$ ), whereas a crystalloid medium without energy substrates (for instance mitochondrial respiration medium, MiR05 [31]) yields the state of ROUTINE respiration with endogenous substrates ( $C_{ER}$ ). In the latter case, the effect of an intracellular formulation of ion composition on cell respiration must be evaluated. No differences in ROUTINE respiration of

intact endothelial cells are observed in culture medium and mitochondrial medium [18]. In mitochondrial medium, the PC protocol can be extended to obtain a measure of enzyme activity of cytochrome *c* oxidase in the presence of TMPD+ascorbate, which increases after permeabilization of the plasma membrane [20].

Application of cell culture medium for respiratory measurements is advantageous when aiming at near-physiological conditions of intact cells. All inhibitors and the uncoupler applied in this protocol are freely permeable through the intact plasma membrane and therefore do not require plasma membrane permeabilization [16]. The PC protocol takes about 90 min (Figure 2 and 6B).

#### 4.1. Titration Steps of the PC Protocol

1. A 10-min period of routine respiration, reflecting the aerobic metabolic activity in the physiological ROUTINE state, *R*.

2. Nonphosphorylating (oligomycin-inhibited) LEAK rate of respiration, caused mainly by compensation for the proton leak after inhibition of ATP synthase (state *L*). Analogous to ADP limitation of respiration in State 4 [34], inhibition of ATP synthase (Complex V) by oligomycin (1 µg/ml) or inhibition of adenylate translocase by atractyloside, arrests mitochondrial respiration at a resting level. Oxygen flux measured in this LEAK state reflects (a) proton leak or futile respiration at maximum mitochondrial membrane potential, which is the main component, (b) proton or electron slip (decoupled respiration which includes electrons diverted away towards reactive oxygen species (ROS) production), (c) cation cycling ( $\text{Ca}^{2+}$ ,  $\text{K}^+$ ), and (d) correction should be made for residual oxygen consumption (ROX), including peroxidase and oxidase activities which partially contribute to ROS production.

3. Uncoupler titration with the titration-injection micropump, which yields the maximum stimulated respiration as a measure of the capacity of the electron transport system (ETS) in nonpermeabilized cells (state *E*), and quantitatively describes the dependence of respiration on uncoupler concentration (Figure 2). The addition of uncouplers, such as the protonophores carbonyl cyanide *p*-trifluoromethoxyphenylhydrazone (FCCP) or DNP induces a state of maximum uncoupled respiration. Uncouplers dissipate the mitochondrial membrane potential and so maximally activate the electron transport system. Uncoupler titrations must be performed carefully, since optimum uncoupler concentrations have to be applied to achieve maximum stimulation of flux, avoiding over-titration, which paradoxically, inhibits respiration [40]. Optimum uncoupler concentrations depend on the cell type, cell concentration, medium, and are different in permeabilized versus intact cells. The release of mitochondrial respiratory control by the phosphorylation system in the uncoupled state compared to the maximum inhibition of respiration achieved through blocking ATP synthesis by oligomycin leads to information on potential respiratory control by coupling as expressed by the respiratory control ratio, RCR (= ratio of respiration in the uncoupled state over respiration in the presence of oligomycin [12]). A possible influence on uncoupled flux by prior inhibition of phosphorylation should be checked by controls in the absence of oligomycin.

4. Rotenone+antimycin A-inhibited respiration after inhibition of complex I and III (residual oxygen consumption, ROX; Figure 6). Mitochondria contribute to residual oxygen consumption (particularly related to ROS production) after inhibition of Complexes I and III, which argues against correcting respiration in states *R*, *L* and *E* for the residual observed after inhibition with rotenone and antimycin A [16-20]. Uncoupling prior to inhibition by rotenone and antimycin A, however, prevents the large increase in mitochondrial ROS production known to occur in the presence of rotenone, and particularly antimycin A, in isolated coupled mitochondria [41;42]. Further inhibition of residual respiration by cyanide may be related to

specific inhibition of cytochrome *c* oxidase, but may also be due to inhibition of cyanide sensitive oxygen consuming enzymes.

#### 4.2. Experimental Example for the PC Protocol

To illustrate the precision of high-resolution respirometry, superimposed plots of oxygen consumption and oxygen concentration from the two O2k chambers with identical cell densities are shown in Figure 2. The low standard deviation of the results (Figure 6A; Table 1) is a measure of methodological variability using subsamples from the same culture flask, whereas cell physiological variability is larger between cultures grown on different days. Highest accuracy is achieved by step titrations of small volumes of uncoupler. The titration is terminated when a small increase in uncoupler concentration does not yield a further stimulation of oxygen flux. The OROBOROS titration-injection micropump TIP-2k provides an accurate and convenient tool for automatic performance of such step-titrations (Figure 2). Two Hamilton syringes with 27 mm needle length and 0.09 mm needle inner diameter are mounted on the TIP-2k for simultaneous titrations into the two O2k chambers.

After an aerobic-anoxic transition (Figure 2A), the two chambers were reoxygenated to different levels, and recording of respiration was continued with manual titrations of rotenone (0.5  $\mu$ M) and antimycin A (2.5  $\mu$ M; Figure 6B). This residual oxygen consumption (ROX) is 9 % of ROUTINE respiration, but 34 and 3 % of states LEAK and ETS (Figure 6A). Residual respiration after inhibition by rotenone and antimycin A is significantly lower in permeabilized cells, suggesting that the major contribution to residual respiration is not due to mitochondria (which remain intact after cell membrane permeabilization), but rather to nonmitochondrial, cellular oxygen consuming processes [8]. Cell respiration in various states was corrected for ROX (Table 1).

**TABLE 1 Metabolic States and Flux Control Ratios in the Phosphorylation Control Protocol with Intact Cells<sup>a</sup>**

| Metabolic State                  | Additions                    | Flux Control Ratio        | Definition                         | Mean $\pm$ SD   |
|----------------------------------|------------------------------|---------------------------|------------------------------------|-----------------|
| ETS, <i>E</i>                    | FCCP                         |                           | Reference state                    |                 |
| ROUTINE, <i>R</i>                | None                         | <i>R/E</i>                |                                    | 0.39 $\pm$ 0.02 |
| LEAK, <i>L</i>                   | Oligomycin,<br>Atractyloside | <i>L/E</i>                |                                    | 0.10 $\pm$ 0.02 |
| netROUTINE, net <i>R/E</i>       |                              | net <i>R/E</i>            | = ( <i>R-L</i> ) / <i>E</i>        | 0.29 $\pm$ 0.02 |
| Residual oxygen consumption, ROX | Rotenone +<br>Antimycin A    | ROX/ <i>E'</i>            |                                    | 0.03 $\pm$ 0.01 |
|                                  |                              | Uncoupling control ratio  | UCR = ( <i>R/E</i> ) <sup>-1</sup> | 2.6 $\pm$ 0.1   |
|                                  |                              | Respiratory control ratio | RCR = ( <i>L/E</i> ) <sup>-1</sup> | 10.1 $\pm$ 1.8  |

<sup>a</sup>Capacity for electron transport is the reference for normalization,  $E = E' - \text{ROX}$ , where  $E'$  is the apparent (uncorrected) electron transport capacity. Mean  $\pm$  standard deviation of six replicate O2k measurements with 32D cells (from Figure 6).

### 4.3. Flux Control Ratios from the PC Protocol

Normalized fluxes are expressed as ratios relative to a common reference state. When the capacity of the electron transport system (ETS) in uncoupled respiration,  $E$ , is chosen as the reference state, normalized fluxes in the PC protocol have the boundaries from 0.0 to 1.0 (Table 1). If the protocol is extended by measurement of cytochrome  $c$  oxidase, then the ratio of CcOX activity and uncoupled respiration is an index of the apparent excess capacity of this enzyme step in the pathway [20].

Routine respiration of 32D cells [12,43] operates at 0.39 of ETS capacity, as expressed by the  $R/E$  ratio of 0.39. 0.29 ETS capacity is used for oxidative phosphorylation under routine conditions (net $R/E$ ; Table 1). If mild uncoupling leads to a parallel increase of  $R/E$  and  $L/E$ , the normalized net routine respiration, net $R/E$ , remains unchanged (e.g. in senescent fibroblasts at 0.2 [16]). The  $R/E$  ratio is  $<1.0$  when cells respire below their ETS capacity. But even at full activation of  $OXPHOS$ , the  $R/E$  ratio remains  $<1.0$ , if the activity of the phosphorylation system (adenine nucleotide translocator, phosphate transporter and ATP synthase) limits maximum coupled flux relative to the maximum ETS capacity. This requires evaluation of the uncoupling effect on ADP-activated respiration (State 3) in isolated mitochondria or permeabilized cells [12,44].

The inverse values of the ROUTINE and LEAK flux control ratios are the uncoupling control ratio, UCR (2.6), and respiratory control ratio, RCR (10.1; Table 1). These conventional inverse ratios are mathematically less convenient, since the RCR has awkward boundaries from 1.0 (fully uncoupled) to infinity (zero LEAK), compared to the  $L/E$  ratio with boundaries from 0.0 (zero LEAK) to 1.0 (fully uncoupled).

The low  $R/E$  flux control ratio indicates a high apparent excess capacity of respiratory complexes (including CcOX) in the parental hematopoietic 32D cells. These results from cells grown and measured in suspension are in agreement with respiratory control in lymphoblastoma cells [20], and with various attached cell types grown in monolayers but evaluated using high-resolution respirometry in suspension, including human umbilical vein endothelial cells [17,40,45], transformed endothelial EA.hyb 926 cells [18], human fibroblasts [9,16], and mesenchymal cells [46]. The reason for lower uncoupling control ratios reported by Villani and Attardi [47,48] is not clear.

Interpretation of respiratory flux control ratios is complicated if drug toxicity causes multiple mitochondrial defects. An increase in the  $L/E$  flux control ratio can be caused not only by uncoupling, but by a decrease of respiratory capacity. Diagnostic protocols for separating these effects in permeabilized muscle fibers are discussed elsewhere [13].

## 5. INTACT CELLS, PERMEABILIZED CELLS AND TISSUE, OR ISOLATED MITOCHONDRIA

Depending on the experimental sample, the rate of oxygen consumption is frequently expressed per million cells, per milligram of tissue (wet or dry weight), per milligram of mitochondrial protein, or per unit of a mitochondrial marker. It is important to note that interpretation of changes in respiratory flux is very different when expressed as per million cells, per mass of cells or tissue, or per mitochondrial marker [20]. For direct comparison of results, a common marker has to be quantified, such as mitochondrial DNA [15], citrate synthase activity [49], CcOX activity [20], or cytochrome  $aa3$  content [50]. Subsamples or the entire contents can be collected from the O2k chamber for analysis of cell count and viability, protein concentration, and enzyme assays (e.g. Complex I, CS and LDH). Normalized flux ratios (Table 1) are, however, independent of the choice of normalization mode and of errors in the quantities chosen as a basis of expressing respiratory flux.

## 5.1. Intact Cells

Taken together, the phosphorylation control assay provides a standardized protocol to assess mitochondrial function in cell-culture-based model systems suitable for drug testing (Figure 6). A particular advantage of studying intact cells is the quantification of respiration in the physiologically controlled state (ROUTINE) in response to intracellular inhibitors or activators of respiration, the availability of substrates and ions (e.g.  $\text{Ca}^{2+}$ ) at physiological combinations, concentrations and spacial distributions, and the avoidance of potential artifacts caused by mitochondrial isolation or cell permeabilization. For analysis of the mechanism of a mitochondrial defect, however, the intact cell poses limitations on assessment of maximum *OXPPOS* capacity in the coupled state, because ADP does not pass through the cell membrane, and on functional assays of various components of the respiratory system, because several substrates do not enter the cell. Extended analyses require either isolation of mitochondria, or selective cell membrane permeabilization by mild detergents, such as digitonin or saponin [13,15,18,51]. Whereas isolated mitochondria remain one of the gold standards in studies of bioenergetics and mitochondrial physiology, permeabilized tissues and cells are an established alternative offering several advantages. However, some disadvantages have to be considered for optimum experimental design and critical evaluation of results.

## 5.2. Permeabilized Cells and Tissue

When comparing results with high specific fluxes and correspondingly high quality control, respiratory activity in permeabilized human skeletal muscle fibers is in accord with isolated mitochondria [52]. With cell membrane permeabilization, fewer cells or less tissue are required than with isolated mitochondria. Using the OROBOROS Oxygraph-2k, 1 mg wet weight of cardiac fibers or 0.3 million fibroblasts or endothelial cells per experimental test are sufficient using a 2-mL chamber at 37 °C. Optimization of mitochondrial isolation is more time-consuming than the optimization of cell membrane permeabilization that is done via standardized protocols.

The degree of mechanical tissue separation may be evaluated by observing a change in the pale colouring of the separated fiber bundles (similar for liver). This is best observed when placing the petri dish onto a dark background. Appropriate forceps have to be used. Initially, the main difficulty is application of excess tissue, which makes mechanical separation of small amounts of tissue tedious (for isolated mitochondria, cf. [52]). A practical quantity for routine experiments is 10 to 12 mg wet weight of tissue, subsequently separated into 2-mg samples for parallel experiments. The mechanical tissue preparation leads to partial (skeletal muscle) or full permeabilization of the cell membrane (heart muscle [13]; liver tissue [49]). A preparation of fully intact cells for the study of routine respiration cannot be obtained by this approach. Partially permeabilized preparations need additional chemical permeabilization by saponin or digitonin [13,51], and via standardized incubation conditions that leave the outer and inner mitochondrial membranes intact. In merely mechanical permeabilized tissue, full permeabilization must be checked by addition of saponin or digitonin to the respirometer during State 3 with succinate+rotenone. Under these conditions, no stimulation of respiration is expected in fully permeabilized cells, whereas partial permeabilization is indicated by the stimulatory effect of added detergent [53].

ADP has to be added to permeabilized cells at high concentrations to achieve maximum State 3 respiration, due to diffusion restrictions and because the outer membrane may exert a barrier different from isolated mitochondria [5,51]. Low oxygen levels have to be strictly avoided in studies with muscle fibers, due to a 100-fold higher oxygen sensitivity in fibers compared to isolated mitochondria [8].

Stability of the tissue preparation in the respirometer at 37 °C depends on the application of a high-quality mitochondrial respiration medium [31], and in isolated mitochondria the isolation and preservation media need to be considered carefully [31,54]. High stability allows for application of complex and extended substrate-uncoupler-inhibitor titration protocols [13,15,55].

All types of mitochondria are accessible experimentally in permeabilized cells and tissues, whereas preparation of isolated mitochondria offers the advantage of separation of different mitochondrial populations. It is generally held but not well documented, that isolation of mitochondria may involve the selective loss of damaged mitochondria, thereby confounding extension of ex vivo data with in vivo circumstances.

### 5.3. Isolated Mitochondria

Isolated mitochondria are required for separation and respirometric study of different mitochondrial subpopulations [56,57]. The homogeneous suspension of isolated mitochondria yields a representative average for the tissue sample, and fewer replica are required for averaging over heterogeneous subsamples of fibers. The oxygen dependence of respiration in permeabilized muscle fibers is increased by two orders of magnitude, due to oxygen diffusion to the mitochondria in the small unperfused fiber bundle. Isolated mitochondria are, therefore, the choice for the study of mitochondrial oxygen kinetics, although small isolated cells are a good model, as well [4-9].

## 6. TITRATION PROTOCOLS IN PERMEABILIZED CELLS, PERMEABILIZED TISSUE PREPARATIONS, AND ISOLATED MITOCHONDRIA

By using either NADH-linked substrates (pyruvate+malate; glutamate+malate) or the classical succinate+rotenone combination, different segments of the electron transport system can be interrogated [12,34]. Mitochondrial respiration depends on a continuous flow of substrates across the mitochondrial membranes into the matrix space. Many substrates are strong anions that cannot permeate lipid membranes and hence require carriers. Various anion carriers in the inner mitochondrial membrane are involved in the transport of mitochondrial metabolites. Their distribution across the mitochondrial membrane varies mainly with  $\Delta\text{pH}$  and not  $\Delta\psi$ , since most carriers (but not the glutamate-aspartate carrier) operate non-electrogenically by anion exchange or cotransport of protons. Depending on the concentration gradients, these carriers also allow for the transport of mitochondrial metabolites from the mitochondria into the cytosol and for the loss of intermediary metabolites into the incubation medium. Export of intermediates of the tricarboxylic acid (TCA) cycle plays an important metabolic role in the intact cell. This must be considered when interpreting the effect on respiration of specific substrates used in studies of isolated mitochondria. Substrate combinations of pyruvate+malate (PM) and glutamate+malate (GM) activate dehydrogenases yielding reduced nicotinamide adenine dinucleotide (NADH), which feeds electrons into Complex I (NADH-ubiquinone oxidoreductase) and hence down the thermodynamic cascade through the Q-cycle and Complex III to Complex IV and ultimately  $\text{O}_2$ .

Complex II is the only membrane-bound enzyme in the tricarboxylic acid cycle and is part of the mitochondrial electron transport chain. The flavoprotein succinate dehydrogenase is the largest polypeptide of Complex II, located on the matrix face of the inner mitochondrial membrane. Following succinate oxidation, the enzyme transfers electrons directly to the quinone pool [58]. Whereas Complex I is NADH-linked *upstream* to the dehydrogenases of

the tricarboxylic acid cycle, Complex II is FADH<sub>2</sub>-linked *downstream* with subsequent electron flow to CoQ [12].

Electrons flow to oxygen from either Complex I, with a total of three proton pumps in series, or from Complex II and other flavoproteins, providing multiple entries into the Q-cycle with only two proton pumps downstream. Substrate combinations that match physiological intracellular conditions are required for evaluation of the maximum capacity of oxidative phosphorylation. A novel perspective of mitochondrial physiology and respiratory control by simultaneous supply of various substrates emerged from a series of studies based on high-resolution respirometry [12,15,19,59]. Application of substrate combinations in multiple substrate-uncoupler-inhibitor titration protocols extends conventional bioenergetic studies to the level of mitochondrial physiology suitable for full characterization of respiratory control in health and disease.

## 7. MULTISENSOR APPLICATIONS

The large chamber of the Oxygraph-2k (16 mm in diameter) offers the possibility of inserting additional sensors into the chamber through the stopper. The signal can be fed into the multichannel electronics of the O2k, providing simultaneous recordings in the DatLab software. Of particular diagnostic value is the simultaneous measurement of respiration and mitochondrial membrane potential [60], using an ion-selective electrode that responds to TPP<sup>+</sup> or TPMP<sup>+</sup> [61,62]. The simultaneous measurement of oxygen consumption and cellular proton production offers a potential for real-time monitoring of aerobic and anaerobic metabolism in intact cells comparable to combined respirometry and microcalorimetry (calorespirometry [6,63,64]). Proton production in conjunction with the enthalpy of neutralization requires consideration as a correction term in calorimetric determination of anaerobic metabolism [64]. Beyond a mere correction term, the ratio of proton production from acidic endproducts to ATP turnover [65] yields a sensitive estimate of anaerobic metabolism. Combining high-resolution respirometry and measurement of nitric oxide under physiological low oxygen levels yields new insights into the competitive inhibition of CcOX [66]. A variety of multisensor applications, such as ion sensitive electrodes or light guides for spectroscopy or fluorescence protocols, render high-resolution respirometry a powerful technology for detection and parsing drug-induced mitochondrial dysfunction.

## References

1. Dykens JA, Will Y. The significance of mitochondrial toxicity testing in drug development. *Drug Discov. Today*. 2007;12:777-785.
2. Gellerich FN, Mayr JA, Reuter S, Sperl W, Zierz S. The problem of interlab variation in methods for mitochondrial disease diagnosis: enzymatic measurement of respiratory chain complexes. *Mitochondrion*. 2004;4:427-439.
3. Gnaiger E, Forstner H, eds. *Polarographic Oxygen Sensors. Aquatic and Physiological Applications*. New York: Springer-Verlag; 1983.
4. Gnaiger E, Steinlechner-Maran R, Méndez G, Eberl T, Margreiter R. Control of mitochondrial and cellular respiration by oxygen. *J Bioenerg Biomembr*. 1995;27:583-596.
5. Gnaiger E. Bioenergetics at low oxygen: dependence of respiration and phosphorylation on oxygen and adenosine diphosphate supply. *Respir Physiol*. 2001;128:277-297.
6. Gnaiger E, Méndez G, Hand SC High phosphorylation efficiency and depression of uncoupled respiration in mitochondria under hypoxia. *Proc Natl Acad Sci USA*. 2000;97: 11080-11085.

7. Gnaiger E, Kuznetsov AV. Mitochondrial respiration at low levels of oxygen and cytochrome c. *Biochem Soc Trans.* 2002;30:252-258.
8. Gnaiger E. Oxygen conformance of cellular respiration: a perspective of mitochondrial physiology. *Adv Exp Med Biol.* 2003;543:39-56.
9. Pecina P, Gnaiger E, Zeman J, Pronicka E, Houštek J. Decreased affinity to oxygen of cytochrome c oxidase in Leigh syndrome caused by SURF1 mutations. *Am J Physiol Cell Physiol.* 2004;287:C1384-C1388.
10. Rostrup M, Fossbakk A, Hauge A, Kleppe R, Gnaiger E, Haavik J. Oxygen dependence of tyrosine hydroxylase. *Amino Acids* 2008;34:455-464.
11. Puchowicz MA, Varnes ME, Cohen BH, Frieman NR, Kerr DS, Hoppel CL. Oxidative phosphorylation analysis: assessing the integrated functional activity of human skeletal muscle mitochondria – case studies. *Mitochondrion.* 2004;4:377-385.
12. Gnaiger E, editor. Mitochondrial pathways and respiratory control. Innsbruck: OROBOROS MiPNet Publications; 2007. <http://www.oroboros.at>
13. Kuznetsov AV, Schneeberger S, Seiler R, Brandacher G, Mark W, Steurer W, Saks V, Usson Y, Margreiter R, Gnaiger E. Mitochondrial defects and heterogeneous cytochrome c release after cardiac cold ischemia and reperfusion. *Am J Physiol Heart Circ Physiol.* 2004;286:H1633–H1641.
14. Wenchich L, Drahotal Z, Honzík T, et al. Polarographic evaluation of mitochondrial enzymes activity in isolated mitochondria and in permeabilized human muscle cells with inherited mitochondrial defects. *Physiol Res.* 2003;52:781-788.
15. Boushel R, Gnaiger E, Schjerling P, Skovbro M, Kraunsøe R, Dela F. Patients with Type 2 Diabetes have normal mitochondrial function in skeletal muscle. *Diabetologia.* 2007;50:790-796.
16. Hütter E, Renner K, Pfister G, Stöckl P, Jansen-Dürr P, Gnaiger E. Senescence-associated changes in respiration and oxidative phosphorylation in primary human fibroblasts. *Biochem J.* 2004;380:919-928.
17. Hütter E, Unterluggauer H, Garedew A, Jansen-Dürr P, Gnaiger E. High-resolution respirometry - a modern tool in aging research. *Exp Gerontol.* 2006;41:103-109.
18. Stadlmann S, Rieger G, Amberger A, Kuznetsov AV, Margreiter R, Gnaiger E. H<sub>2</sub>O<sub>2</sub>-mediated oxidative stress versus cold ischemia-reperfusion: mitochondrial respiratory defects in cultured human endothelial cells. *Transplantation.* 2002;74:1800-1803.
19. Aragonés J, Schneider M, Van Geyte K, et al. Deficiency or inhibition of oxygen sensor Phd1 induces hypoxia tolerance by reprogramming basal metabolism. *Nature Genetics* 2008;40:170-180.
20. Renner K, Amberger A, Konwalinka G, Kofler R, Gnaiger E. Changes of mitochondrial respiration, mitochondrial content and cell size after induction of apoptosis in leukemia cells. *Biochim Biophys Acta* 2003;1642:115-123.
21. Hofhaus G, Shakeley RM, Attardi G. Use of polarography to detect respiration defects in cell cultures. *Methods Enzymol.* 1996;264:476-83.
22. Yamaguchi R, Andreyev A, Murphy AN, Perkins GA, Ellisman MH, Newmeyer DD. Mitochondria frozen with trehalose retain a number of biological functions and preserve outer membrane integrity. *Cell Death Differentiation.* 2006;14:616-624.
23. Frezza C, Cipolat S, Scorrano L. Organelle isolation: functional mitochondria from mouse liver, muscle and cultured fibroblasts. *Nat Protoc.* 2007;2:287-295.
24. Villani G, Attardi G. Polarographic assays of respiratory chain complex activity. *Methods Cell Biol.* 2007;80:121-133.
25. Renner K, Kofler R, Gnaiger E. Mitochondrial function in glucocorticoid triggered T-ALL cells with transgenic Bcl-2 expression. *Molec Biol Rep.* 2002;29:97-101.
26. Holtzmann D, Moore CL A micro-method for the study of oxidative phosphorylation. *Biochim Biophys Acta.* 1971;234:1-8.

27. Atkinson HJ, Smith L. An oxygen electrode microrespirometer. *J Exp Biol.* 1973;59:247-253
28. Suchy J, Cooper C. Isolation and respiratory measurement on a single large mitochondrion. *Experimental Cell Res.* 1974;88:198-202.
29. Justice RE, Utsunomiya T, Krausz MM, Valeri CR, Shepro D, Hechtman HB. A miniaturized chamber for the measure of oxygen consumption. *J Appl Physiol.* 1982;52:488-490.
30. Rasmussen HN, Rasmussen UF. Respiration measurements in small scale. *Anal Biochem.* 1993;208:244-248.
31. Gnaiger E, Kuznetsov AV, Schneeberger S, Seiler R, Brandacher G, Steurer W, Margreiter R. Mitochondria in the cold. In *Life in the Cold* (G Heldmaier, M Klingenspor, eds). New York: Springer-Verlag, 2000:431-442.
32. Rasmussen HN, Rasmussen UF. Oxygen solubilities of media used in electrochemical respiration measurements. *Anal Biochem.* 2003;319:105-113.
33. Baumgärtl H, Lübbers DW. Microaxial needle sensor for polarographic measurement of local O<sub>2</sub> pressure in the cellular range of living tissue. Its construction and properties. In *Polarographic Oxygen Sensors* (E Gnaiger, H Forstner, eds). New York: Springer-Verlag, 1983:37-65.
34. Chance B, Williams GR. Respiratory enzymes in oxidative phosphorylation. I. Kinetics of oxygen utilization. *J Biol Chem.* 1955;217:383-393.
35. Lemasters JJ. The ATP-to-oxygen stoichiometries of oxidative phosphorylation by rat liver mitochondria. *J Biol Chem.* 1984;259:13123-13130.
36. Stoner CD. Determination of the P/2e<sup>-</sup> stoichiometries at the individual coupling sites in mitochondrial oxidative phosphorylation. *J Biol Chem.* 1987;262:11445-11453.
37. Robiolio M, Rumsey WL, Wilson DF. Oxygen diffusion and mitochondrial respiration in neuroblastoma cells. *Am J Physiol.* 1989;256:C1207-C1213.
38. Hollis VS, Palacios-Callender M, Springett RJ, Delpy DT, Moncada S. Monitoring cytochrome redox changes in the mitochondria of intact cells using multi-wavelength visible light spectroscopy. *Biochim Biophys Acta* 2003;1607:191-202.
39. Garedew A, Hütter E, Haffner B, Gradl P, Gradl L, Jansen-Dürr P, Gnaiger E. High-resolution respirometry for the study of mitochondrial function in health and disease. The OROBOROS Oxygraph-2k. Proceedings of the 11th Congress of the European Shock Society, Vienna, Austria (H Redl, ed) Bologna, Italy: Medimond International Proceedings,; 2005:107-111.
40. Steinlechner-Maran R, Eberl T, Kunc M, Margreiter R, Gnaiger E. Oxygen dependence of respiration in coupled and uncoupled endothelial cells. *Am J Physiol.* 1996;271:C2053-C2061.
41. Boveris A, Chance B. The mitochondrial generation of hydrogen peroxide. General properties and effect of hyperbaric oxygen. *Biochem J.* 1973;134:707-716.
42. Garait B, Couturier K, Servais S, Letexier D, Perrin D, Batandier C, Rouanet J-L, Sibille B, Rey B, Leverve X, Favier R. Fat intake reverses the beneficial effects of low caloric intake on skeletal muscle mitochondrial H<sub>2</sub>O<sub>2</sub> production. *Free Radic Biol Med.* 2005;39:1249-1261.
43. Troppmair J, Rapp UR. Raf and the road to cell survival: a tale of bad spells, ring bearers and detours. *Biochem Pharmacol.* 2003;66:1341-1345.
44. Rasmussen UF, Rasmussen HN, Krstrup P, Quistorff B, Saltin B, Bangsbo J. Aerobic metabolism of human quadriceps muscle: in vivo data parallel measurements on isolated mitochondria. *Am J Physiol Endocrinol Metab.* 2001;280:E301-E307.
45. Steinlechner-Maran R, Eberl T, Kunc M, Schröcksnadel H, Margreiter R, Gnaiger E. Respiratory defect as an early event in preservation/reoxygenation injury in endothelial cells. *Transplantation.* 1997;63:136-142.

46. Stadlmann S, Renner K, Pollheimer J, Moser PL, Zeimet AG, Offner FA, Gnaiger E. Preserved coupling of oxydative phosphorylation but decreased mitochondrial respiratory capacity in IL-1 $\beta$  treated human peritoneal mesothelial cells. *Cell Biochem Biophys*. 2006;44:179-186.
47. Villani G, Attardi G. In vivo control of respiration by cytochrome c oxidase in wild-type and mitochondrial DNA mutation-carrying human cells. *Proc Natl Acad Sci USA*. 1997;94:1166-1171.
48. Villani G, Greco M, Papa S, Attardi G. Low reserve capacity of cytochrome c oxidase capacity in vivo in the respiratory chain of a variety of human cell types. *J Biol Chem*. 1998;273:31829-31836.
49. Kuznetsov AV, Strobl D, Ruttman E, Königsrainer A, Margreiter R, Gnaiger E. Evaluation of mitochondrial respiratory function in small biopsies of liver. *Anal Biochem*. 2002;305:186-194.
50. Mootha VK, Arai AE, Balaban RS. Maximum oxidative phosphorylation capacity of the mammalian heart. *Am J Physiol*. 1997;272:H769-H775.
51. Saks VA, Veksler VI, Kuznetsov AV, Kay L, Sikk P, Tiivel T, Tranqui L, Olivares J, Winkler K, Wiedemann F, Kunz WS. Permeabilised cell and skinned fiber techniques in studies of mitochondrial function in vivo. *Mol Cell Biochem*. 1998;184:81-100.
52. Rasmussen UF, Rasmussen HN. Human quadriceps muscle mitochondria: A functional characterization. *Mol Cell Biochem*. 2000;208:37-44.
53. Gnaiger E, Kuznetsov AV, Lassnig B, et al. High-resolution respirometry. Optimum permeabilization of the cell membrane by digitonin. In *BioThermoKinetics in the Post Genomic Era* (C Larsson, I-L Pålman, L Gustafsson, eds). Göteborg, Sweden: Chalmers Reproservice; 1998:89-95.
54. Brewer GJ, Jones TT, Wallimann T, Schlattner U. Higher respiratory rates and improved creatine stimulation in brain mitochondria isolated with anti-oxidants. *Mitochondrion*. 2004;4:49-57.
55. Gnaiger E, Wright-Paradis C, Sondergaard H, et al. High-resolution respirometry in small biopsies of human muscle: correlations with body mass index and age. *Mitochondr Physiol Network*. 2005;10(9):14-15. <http://www.mitophysiology.org/index.php?gnaigere>.
56. Palmer JW, Tandler B, Hoppel CL. Biochemical properties of subsarcolemmal and interfibrillar mitochondria isolated from rat cardiac muscle. *J Biol Chem*. 1977;252:8731-8739.
57. Riva A, Tandler B, Loffredo F, Vazquez E, Hoppel CL. Structural differences in twobiochemically defined populations of cardiac mitochondria. *Am J Physiol Heart Circ Physiol*. 2005;289:H868-H872.
58. Sun F, Huo X, Zhai Y, Wang A, Xu J, Su D, Bartlam M, Rao Z. Crystal structure of mitochondrial respiratory membrane protein Complex II. *Cell*. 2005;121:1043-1057.
59. Lemieux H, Garedew A, Blier PU, Tardif J-C, Gnaiger E. Temperature effects on the control and capacity of mitochondrial respiration in permeabilized fibers of the mouse heart. *Biochim Biophys Acta (EBEC Short Rep Suppl)*. 2006;14:201-202.
60. Jekabsons MB, Nicholls DG. In situ respiration and bioenergetic status of mitochondria in primary cerebellar granule neuronal cultures exposed continuously to glutamate. *J Biol Chem*. 2004;279:32989-33000.
61. Brand MD. Measurement of mitochondrial protonmotive force. In *Bioenergetics - A Practical Approach* (GC Brown, CE Cooper, eds).. New York: Oxford University Press; 1995.
62. Labajova A, Vojtiskova A, Krivakova P, Kofranek J, Drahota Z, Houstek J. Evaluation of mitochondrial membrane potential using a computerized device with a tetraphenylphosphonium-selective electrode. *Anal Biochem*. 2006;353:37-42.

63. Gnaiger E. The twin-flow microrespirometer and simultaneous calorimetry. In *Polarographic Oxygen Sensors. Aquatic and Physiological Applications* (E Gnaiger, H Forstner, eds). New York: Springer-Verlag, 1983:134-166.
64. Gnaiger E, Kemp RB. Anaerobic metabolism in aerobic mammalian cells: information from the ratio of calorimetric heat flux and respirometric oxygen flux. *Biochim Biophys Acta*. 1990;1016:328-332.
65. Gnaiger E. Heat dissipation and energetic efficiency in animal anoxibiosis. Economy contra power. *J Exp Zool*. 1983;228:471-490.
66. Aguirre E, Rodriguez-Juarez F, Gnaiger E, Cadenas S. Measurement of the control of cellular respiration by nitric oxide under normoxia and hypoxia: instrumental comparison including high-resolution respirometry. *Biochim Biophys Acta*. (EBEC Short Rep Suppl). 2006;14:136-137.

